QUANTUM EFFICIENCY OF CdTe SOLAR CELLS IN FORWARD BIAS

M. Gloeckler and J. R. Sites
Department of Physics, Colorado State University
Fort Collins, CO 80523-1875 USA
Tel: +1-970-491-6072, Fax: +1-970-491-7947, e-mail: markusg@lamar.colostate.edu

ABSTRACT: When the quantum efficiency of a CdS/CdTe solar cell is measured under forward voltage, the measurement is likely affected by several factors including (1) the voltage dependence of the collection efficiency, (2) series resistance of the cell and instrumentation, (3) the electrical barrier of the back contact, (4) photoconductive effects in the CdS and CdTe, and (5) any secondary barrier in the primary junction. Each of these effects has a distinct signature, but without careful attention to these signatures, misinterpretation is possible and perhaps common. The approach here is to numerically simulate effect (1), and then progressively add effects (2), (3), (4), and (5). In each case, we show the characteristic signature of the apparent quantum efficiency when voltage is varied, we discuss the effect of bias light on the quantum efficiency measurement, we compare when possible with analytical modeling, and we show the impact of each effect on the cell's current-voltage curves, particularly the light/dark crossover. Although the presentation will be specific to CdTe cells, the principles should at least in part apply to other solar cells as well.
Keywords: CdTe, Photoconductivity, Characterisation

1 INTRODUCTION

In this contribution, we use numerical modeling tools to illustrate the effects of collection efficiency, series resistance, photoconductivity, and secondary barriers on the apparent quantum efficiency (AQE) of CdTe solar cells. Earlier analytical work by Phillips and Roy [1] and Sites et al. [2] describes the apparent quantum efficiency under forward bias, and we compare our results with the analytical model where applicable.

Back contact barriers in CdTe generally form blocking Schottky contacts, which can be mitigated by the inclusion of Cu [3]. Back contact effects on AQE were partially modeled by Bätzner et al. [4]. Especially after elevated temperature stress, the CdS buffer layer in CdS/CdTe solar cells is often extremely photoconductive. Modeling calculations have assumed heavily compensated materials [5, 6] or even CdS that becomes intrinsic or p-type [7]. The photoconductivity leads to dependence of the apparent quantum efficiency on light bias [8] and can cause secondary barriers located at the primary junction that result in several observable AQE effects [6].

The reduction of the AQE under forward bias is often misinterpreted as a reduction of the light-generated current $J_L(V)$. Besides the fact that a resistive increase in the forward current typically dominates $J_L(V)$ effects [1, 2], other causes of non-superposition can be misinterpreted as strong $J_L(V)$ effects as well. Numerical simulations, free of any series resistance, are used in Sec. 4 to demonstrate such behavior.

2 DEVICE MODEL

The AQE modeling calculations discussed in the following sections used the software tool AMPS-1D [9]. The device model consists of n^+-type window (SnO_2, 500 nm), n-type buffer (CdS, 100 nm), and p-type absorber (CdTe, 4000 nm). The full selection of input parameters was given in Ref. [10]. Variations on these baseline parameters will be discussed in the following sections. Illumination, unless otherwise specified, is a standard AM1.5 spectrum with a total intensity near 100 mW/cm^2.

3 AQE RESULTS

3.1 Ideal Case (Collection Efficiency)

In an ideal solar cell, with series resistance $R_S = 0$ and other secondary effects negligible, the apparent quantum efficiency is determined by the voltage dependence of the collection efficiency. Under the assumption that only carriers generated in the space charge region are collected, AQE will be zero under flat-band conditions. $V_{flat\text{-}band}$ is determined by the built-in potential and the band offset between n- and p-type semiconductors. The numerical model for this situation was: CdTe baseline case as in Ref. [10], deep defects replaced with recombination centers that have a very low density compared to the shallow dopants and large capture cross-sections, $\sigma_e = \sigma_h$. Hence, there is only negligible charge associated with the deep states, and charge-trapping effects are negligible, but these deep states do provide the path for recombination. This is in many ways comparable to a traditional lifetime model. The back barrier is set to 0.3 eV, and hence negligible. Resulting V_{oc} is near 0.9 V and efficiency about 16%. The ideal J-V curves in the dark and under illumination are shown in Fig. 1. The other curves in the figure relate to series resistance and contact barrier effects that will be discussed below.

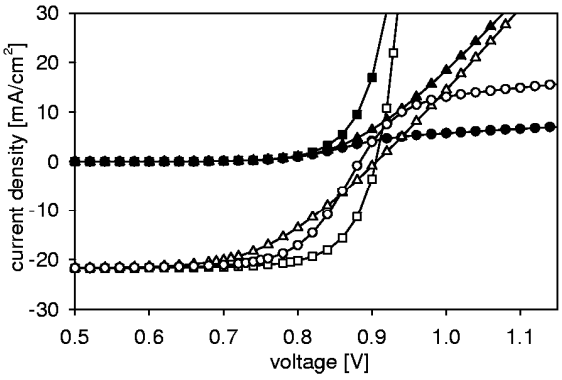

Figure 1: Simulated light and dark J-V curves: ideal cell (squares), significant series resistance (triangles), and significant back contact (circles).

Figure 2 shows the numerical and analytical calculations of AQE as a function of voltage and series resistance. The solid curve corresponds to the ideal curve in Fig. 1 and shows the AQE without series resistance. The numerical model predicts AQE of zero at $V_{flat\text{-}band}$ = 1.07 V and an AQE loss at V_{oc} of less than 5%. In this ideal model it can be assumed that the light generated current, $J_L(V)$, is approximately proportional to the collection efficiency; hence, $J_L(V)$ effects up to V_{oc} can also be expected to be the order of only a few percent [11]. The relations between J-V cross-over, quantum efficiency, and $J_L(V)$ will be discussed further in section 4.

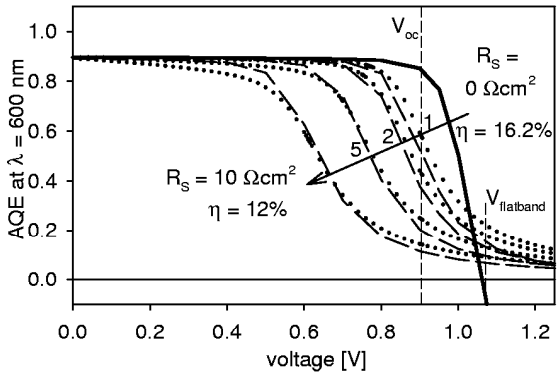

Figure 2: Ideal case without (solid black) and with series resistance (dashed lines). Analytical model (dotted lines).

3.2 Series Resistance

An external resistive layer is used to model the series resistance R_S. This layer has no optical generation, no recombination (defects), and both bands are aligned with the SnO_2 layer. The mobility is set $\mu_e = 1.25 \times 10^{-3}$ cm^2/Vs. R_S values of 1, 2, 5, and 10 Ωcm^2 are simulated. The dark and light J-V curves for R_S = 5 Ωcm^2 are shown in Fig. 1, and the AQE response at λ = 600 nm for the various values of R_S is depicted in Fig. 2. Analytical work by Sites et al. [2] showed that AQE(V) follows the relation

$$AQE(V) = \left(1 + J_F R_S / AkT\right)^{-1} \qquad (1)$$

which is shown for comparison in Fig 2. A is the diode quality factor and J_F is the diode forward current. The shunt term in the expression from Ref. [2] is negligible. The AQE response drops significantly before the voltage reaches V_{oc}. At V_{oc} the AQE losses are 37%, 55%, 69%, and 78% respectively for series resistances of 1, 2, 5, and 10 Ωcm^2. Hence, the changes in AQE due to series resistance are much greater than the small effect due to the collection efficiency variation. It was shown before, that similar good agreement is found when the analytical model is compared to experimental data from Si, CdTe, or $CuInSe_2$ solar cells [2].

3.3 Back-Contact Collection

CdTe solar cells often have a current-limiting Schottky back contact that can cause roll-over of the J-V curves. Although this Schottky diode is located at the back of the device, if the absorber is fairly depleted due to low doping or strong compensation, the back barrier may be ineffective at low voltages and the device behaves much like a n-i-p structure. Our baseline configuration, which we believe reasonably approximates CdTe cells, includes CdTe that is fairly depleted in the dark since deep donors compensate shallow acceptor levels. Under illumination, the compensation is partially lifted which leads to a cross-over of the light and dark J-V curves [10].

AQE at increasing voltages with a significant back barrier (0.5 eV) is shown in Figure 3. The corresponding J-V curves are the circles in Fig. 1.

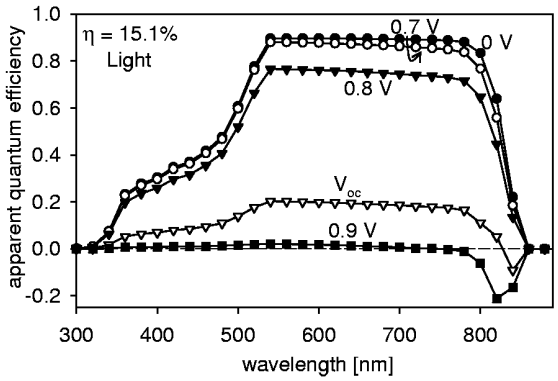

Figure 3: AQE with increasing voltage bias. Small negative band-gap close response.

The conversion efficiency is reduced by about 1%, but AQE at V_{oc} is reduced by more than 50%. By 900 mV, a negative peak appears in the 800 - 850 nm wavelength region, which is due to red photons that penetrate into the back-contact region where the field is opposite to the primary diode field. Only photons with photon energies close to the band gap of the absorber material will penetrate the device and be collected at the back contact. The negative peak height is limited to the fraction of light that is absorbed in the secondary space charge region located at the back of the device.

Partial modeling of this effect has been reported by Bätzner et al. [4]. Agostinelli and Dunlop [12] pointed out that if this secondary space charge region is present at 0V, the negative response may still be present, but is observed as a reduction in the larger positive response for longer wavelength light.

3.4 CdS Photoconductivity

Photoconductivity in the n-type CdS buffer layer can induce cross-over effects in thin film solar cells [13] and other nonidealities in J-V curves [14]. The most direct effects of photoconductivity with CdS/CdTe solar cells are the changes in J-V and AQE results when filtered bias light is used for illumination [8]. The photoconductivity in the CdS can lead to a light-dependent increase in the depletion width of the absorber material as it is depicted in Fig. 4. Blue light, either from the probing beam of the AQE measurement itself or from the dc bias light, significantly increases the depletion width. Under red light bias, the AQE response in the spectral CdS region (λ < 520 nm) can be greatly enhanced since the modulation of the depletion width by the blue probing beam leads to a small modulation of the collection efficiency and, hence, a *small* modulation of the *large* dc red bias light current, shown in Fig. 5. Blue light bias, however, leads to a depletion-width widening, a small increase in the depletion width, and hence, only a small increase in the collection efficiency (AQE) for red

photons in the spectral range $\lambda > 600$ nm. Hegedus et al. [8] reported experimental results and a qualitative explanation of these effects. Detailed modeling information is given elsewhere [6].

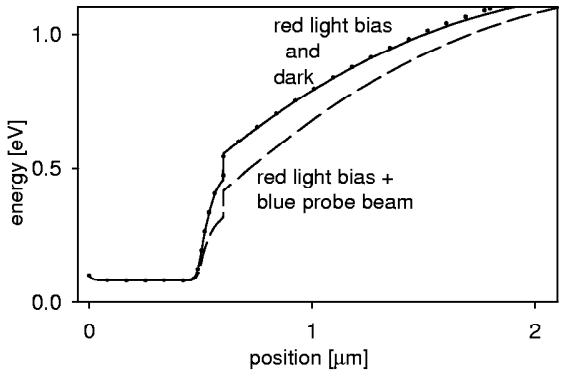

Figure 4: Depletion width change with blue light.

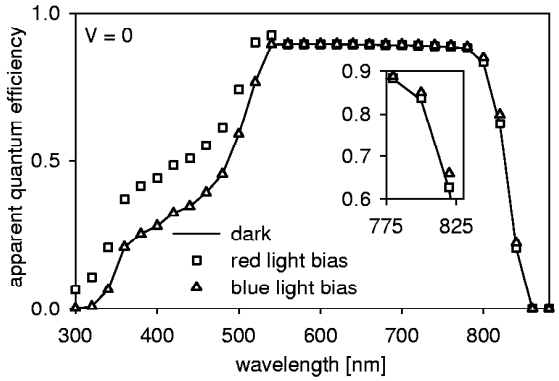

Figure 5: AQE under bias light

3.5 Secondary Barrier Effects

The most dramatic AQE results are achieved with measurements under forward bias in the absence of bias light. Experimental results reported by Bätzner et al. [4] were reproduced with numerical models with very good agreement [8] (see Fig. 6).

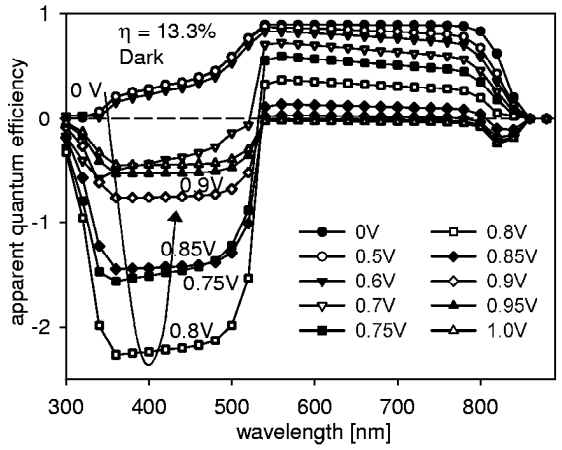

Figure 6: AQE in the dark under forward bias.

The AQE shows two peaks, near 400 and 840 nm, for voltages greater than 0.6 V. Both these peaks were seen experimentally and interpreted as negative due to the large phase shift in the lock-in signal of the AQE measurement. For the low wavelength peak, the signal increases rapidly above 0.6 V, has a maximum at 0.8 V, and decreases at still higher voltages. The peak at 840 nm is caused by a back contact reverse diode as discussed above. The response in the intermediate region (520 nm < λ < 800 nm) behaves similarly to what would be expected from a solar cell with series resistance as discussed in section 3.2. The large negative peak below 500 nm is generated when trapped holes that were generated by blue photons pull down the CdS conduction band and allow considerably more forward current (opposite sign from photocurrent) to flow. The trapping into the acceptor-like trap levels is supported by the unequal capture cross sections, which follow from a consideration of the charge states of the free carriers and the deep states [10]. A full list of input parameter for this calculation is given in Ref. [6].

4 VOLTAGE-DEPENDENT COLLECTION

This last section will focus on the degree of coupling between J-V cross-over and light-dependent collection effects. Ideally, a light J-V curve is the dark curve shifted by the light-generated current. Conversely, one might attempt to calculate the voltage dependence of the light generated current by subtracting the light J-V curve from the dark J-V curve. The collection efficiency, CE, is then assumed to be the ratio of the light generated current at voltage V compared to the absorption limited light generated current, J_{L0}.

$$CE(V) = \frac{J_L(V)}{J_{L0}} = \frac{J_{Light}(V) - J_{Dark}(V)}{J_{L0}} \qquad (2)$$

For well-behaved devices, J_{L0} can often be approximated by the short-circuit current density, otherwise, its value needs to be determined under reverse bias. The reduction of CE from Eq. (2) is sometimes interpreted as evidence for a reduction in $J_L(V)$ under forward bias. Reliable evaluation of $J_L(V)$, however, needs to take other factors into account:

(a) Series Resistance. AQE is dominated by resistive effects under forward bias as it has been discussed in Refs. [1, 2] and reproduced with modeling tools above. Hence, correction of the J-V curves for series resistance is necessary before the true collection efficiency can be extracted. In the case of CdTe solar cells, such correction is further complicated by non-ohmic contacts, which form additional circuit components in series with the main junction. Additionally, attempts to correct for the secondary diode at the back must consider the possibility that the main and secondary diodes may interact unless the absorber is very thick.

(b) Photoconductivity. Any light-induced changes to a photovoltaic diode, i.e. photoconductivity in any of the layers or charge trapping in deep states, invalidate Eq. 2 since some of the diode parameters are altered between dark and light measurements. This complication can be partially avoided using the difference between light curves measured at different light intensities instead of the difference between light and dark curves, as suggested by Hegedus [15]. The collection efficiency can then be written as

$$CE(V) = \frac{J(V,100\%) - J(V,x\%)}{J_{L0}(100\%) - J_{L0}(x\%)} \qquad (3)$$

where J(V, x%) is the current output of the solar cells at a voltage V under illumination x% of AM1.5.

(c) Secondary Barriers. J-V curves of thin film solar cells can be affected in many ways, inducing cross-over, without changing the collection efficiency. This is demonstrated in Fig. 7 where the apparent collection efficiency calculated based on J-V curves using Eq. 3 is displayed. The input parameters were used as those given in Ref. [10].

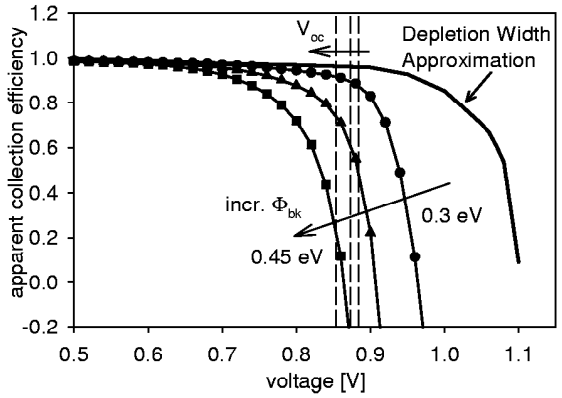

Figure 7: Apparent change in the collection efficiency caused by variations in the back contact barrier, Φ_{bc} = 0.3, 0.4, and 0.45 eV. V_{oc} increases slightly with decreasing Φ_{bk}. In comparison, estimate of the collection efficiency based on depletion width collection.

The only change in the model is the back contact barrier, Φ_{bk}. The front of the junction is unaltered, and V_{oc} only changes slightly. However, the cross-over point of dark and light J-V curves shifts to lower voltages with higher back barriers and, hence, an apparent reduction in $J_L(V)$ is seen. In comparison, the collection efficiency based on the assumption that all electron hole pairs generated in the depletion region are collected (for Φ_{bc} = 0.4 eV) is shown. The depletion region width is determined from the band diagrams of the numerical model. Electric field strength of 100 V/cm is used as cut-off to define the depletion width edge. In all cases, the use of Eq. 3 considerably underestimates CE(V) at V_{oc}, and to a lesser extent at V_{mp}.

5 DISCUSSION AND CONCLUSIONS

Using numerical simulations we have shown that the series resistance of the solar cell dominates the apparent quantum efficiency reduction in forward bias. Secondary barriers and photoconductivity can also significantly alter results and mask the true quantum efficiency or collection efficiency. The current density found by integration over the product of q times Φ times AQE at zero bias, where Φ is the photon flux, usually agrees well with J_{sc} found from J-V measurements. Under forward bias, however, the determination of $J_L(V)$ by this method fails if significant series resistance or secondary barriers play a role in the AQE response. A clear indicator for the presence of secondary barriers is negative AQE response or AQE response above unity. In this case, current response is often highly non-linear with light intensity, and for the AQE effects to appear, the absence of other light is required [6]. Conversely, AQE measurements have the potential to be an useful tool in analyzing solar cells that exhibit irregular characteristics.

The determination of the collection efficiency using current voltage curves fails frequently for thin-film solar cells, since this approach is based on the assumption that cross-over of light and dark J-V curves results only from the voltage dependence of the light generated current. When other effects influence the cross-over, as we have demonstrated with the numerical calculations, invalid results for the collection efficiency may be obtained.

ACKNOWLEDGMENTS

This research was supported by the U.S. National Renewable Energy Laboratory and by the Japanese New Energy Development Organization. The modeling calculation for this work used the AMPS-1D software developed at the Pennsylvania State University by S. Fonash et al. supported by the Electric Power Research Institute.

REFERENCES

[1] J. E. Phillips and M. Roy, in Proc. 20th IEEE Photovoltaic Specialist Conf. (1988), p. 1614.
[2] J. R. Sites, H. Tavakolian, and R. A. Sasala, Solar Cells **29**, 39 (1990).
[3] C. R. Corwine, A. O. Pudov, M. Gloeckler, S. H. Demtsu, and J. R. Sites, Sol. Energy Mat. Sol. Cells **82**, 481 (2004).
[4] D. L. Bätzner, G. Agostinelli, A. Romeo, H. Zogg, and A. N. Tiwari, Mat. Res. Soc. Symp. Proc. **668**, H5.17.1 (2001).
[5] M. Köntges, R. Reineke-Koch, P. Nollet, J. Beier, R. Schäffler, and J. Parisi, Thin Solid Films **403-404**, 280 (2002).
[6] M. Gloeckler and J. R. Sites, J. Appl. Phys. **95**, 4438 (2004).
[7] G. Agostinelli and E. D. Dunlop, Thin Solid Films **431-432**, 448 (2003).
[8] S. Hegedus, D. Ryan, K. Dobson, B. McCandless, and D. Desai, Mat. Res. Soc. Symp. Proc. **763**, 447 (2003).
[9] J. Hou and S. J. Fonash, in Proc. 25th IEEE Photovoltaic Specialist Conf. (1996), p. 961.
[10] M. Gloeckler, A. F. Fahrenbruch, and J. R. Sites, in Proc. 3rd World Conf. Photovoltaic Energy Conversion (2003), 2P–D3–52.
[11] X. X. Liu and J. R. Sites, J. Appl. Phys. **75**, 557 (1994)
[12] G. Agostinelli and E. D. Dunlop, in Proc. 17th European Photovoltaic Sol. Energy Conf. (2001), p. 1054.
[13] M. Gloeckler, C. R. Jenkins, and J. R. Sites, Mat. Res. Soc. Symp. Proc. **763**, 231 (2003).
[14] G. Agostinelli, E. D. Dunlop, D. L. Bätzner, A. N. Tiwari, P. Nollet, M. Burgelman, and M. Köntges, in Proc. 3rd World Conf. Photovoltaic Energy Conversion (2003), 2O–C10–03.
[15] S. S. Hegedus, Prog. Photovoltaics **5**, 151 (1997).